Allosteric Manipulation of Photoexcited State Relaxation in a Series of $Ru^{II}(bpy)_2$(bipyridine−crown ethers)

Subodh K. Dutta,[a] Daqing Gan,[a] and Marc W. Perkovic*[a]

Keywords: Luminescence / Sensors / Photophysics / Lead

A series of ruthenium(II) crown ether complexes containing 4-, 5-, or 6-oxygen crowns tethered to a bipyridine at the 3,3′ position were prepared and examined for their ability to act as luminescent sensors. The complexes $[(bpy)_2Ru(2,2'\text{-bipyridine-}3,3'\text{-}16\text{-crown-}4)](PF_6)_2$ and $[(bpy)_2Ru(2,2'\text{-bipyridine-}3,3'\text{-}19\text{-crown-}5)](PF_6)_2$ were characterized by X-ray crystallography. The 4-oxygen crown crystallizes in the $P\bar{1}$ space group. The 5-oxygen crown crystallizes in the $P\bar{1}$ space group. In both complexes, the inter-pyridine ring angle in the tethered bipyridine is twisted substantially away from 0°. Coordination of a heavy metal ion such as Pb^{2+} by the crown ether, and the geometric changes that result, were examined by UV/Vis, luminescence and NMR spectroscopy. The results show that there is a weak allosteric interaction between the Pb^{2+} ion and the Ru complexes, and that this interaction alters the luminescent behavior of the Ru complexes.
(© Wiley-VCH Verlag GmbH & Co. KGaA, 69451 Weinheim, Germany, 2003)

Introduction

The ability to manipulate the physical and chemical properties of an electronically excited molecule is widely accepted as a necessary component of developing molecular devices. The development of luminescent sensors for a host of analytes has been an active area of research.[2−5] Sensors that are based on coordination complexes of transition metals have been of particular interest.[6] Regardless of the nature of the luminophore, the mechanism by which the act of sensing results in a change in the photophysical behavior of the electronically excited molecule is of particular importance.[7] We have been investigating such mechanisms by examining molecules in which the change in photophysical behavior is the result of geometric perturbations of the transition metal center of the luminophore complex.[8]

When considering the photophysical behavior of transition metal excited state complexes, it is often difficult to distinguish between geometric and electronic effects since the two effects are rarely isolable. For example, to what extent do alterations of the substituents on a ligand effect the electron density on the metal, the electron distribution of the M−L bond, and subsequently the energy and lifetime of the photoexcited state? We have attempted to address this ambiguity by examining a series of complexes based on the well-understood $Ru(bpy)_3{}^{2+}$ molecule, where one of the bipyridine rings has been functionalized at the 3,3′ positions with a crown ether tethered to the bpy pyridine ring.

The oxygen atoms on the crown ethers are not part of the π-system of the bipyridine ligands to any appreciable extent, yet their motion may be telegraphed to the metal center by altering the inter-pyridine ring angle, as has been observed in the complex containing 3,3′-binicotinic acid.[9] Using this approach, we can change the geometry around the metal through an allosteric interaction between the crown ether and the free cations in solution, without changing the ligands.

Results and Discussion

Synthesis and Characterization of the Complexes

The preparation of the Ru(crown-ether) complexes proceeds via facile ligand exchange between the free crown ligands and the chloride ligands of [*cis*-$Ru(bpy)_2Cl_2$]. It has previously been reported that the crown ligands adopt a geometry that is unfavorable for coordination to the ru-

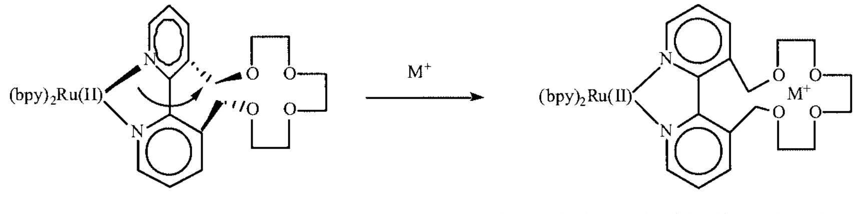

---

[a] Department of Chemistry, Western Michigan University, Kalamazoo, MI 49008, USA
E-mail: perkovic@wmich.edu

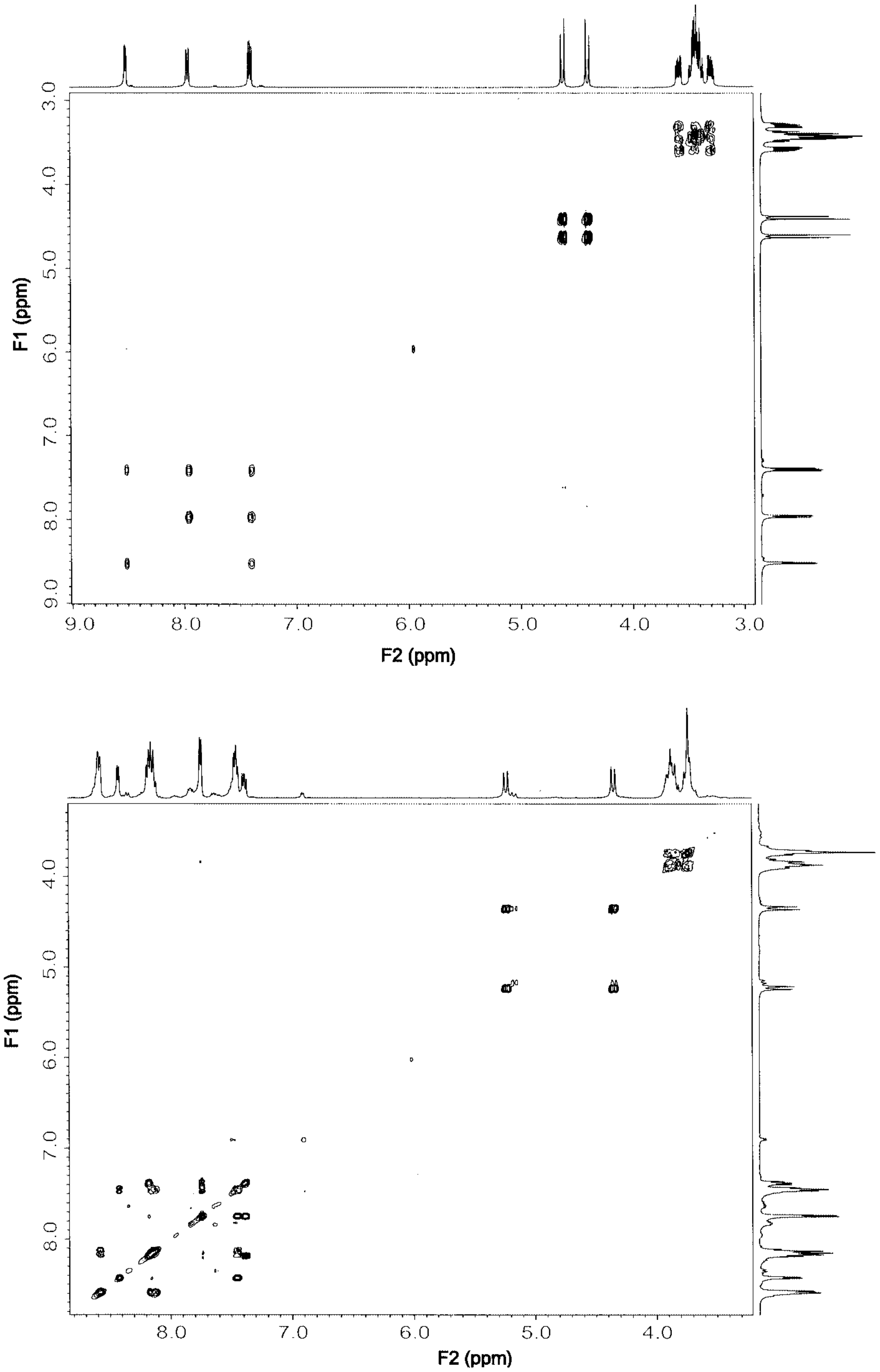

Figure 1. Proton-proton 2D COSY spectrum in CH_3CN of bipyridine-3,3′-16-crown-4 at room temperature (**A**) and $[(bpy)_2Ru(2,2'$-bipyridine-3,3′-16-crown-4)]$(PF_6)_2$ at −20 °C (**B**). Changing the temperature does not alter the chemical shifts, but clarifies the coupling constants for the ruthenium complex

thenium(II) atom, with the coordinating nitrogen atoms on opposite sides of the bipyridine bridge.[15] Complex formation nevertheless readily occurs, resulting in a $[(bpy)_2Ru(crown)]^{2+}$ complex where the inter-pyridine ring angle in the crown tethered bipyridine is substantially twisted away from 0°.[9] The geometric change is reflected

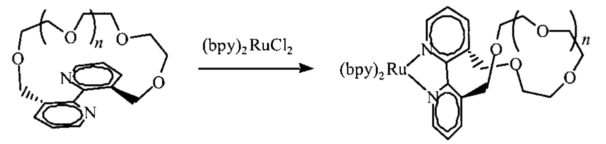

in the NMR spectrum, particularly in the resonances of the correlated benzylic protons at ≈ 5 ppm, as shown in Figure 1. Peak assignments are presented Table 5.

X-ray Structure Determination

X-ray Determination of [(bpy)$_2$Ru(2,2′-bipyridine-3,3′-16-crown-4)](PF$_6$)$_2$

X-ray quality crystals were grown by slow diffusion of diethyl ether into a solution of the crown complex in pyridine. A deep red, rectangular plate, approximately 0.25 × 0.12 × 0.1 mm, was chosen by size, habit, and polarized light microscopy. The complex crystallized in the triclinic system in the space group $P\bar{1}$(#2),[10] as determined from 25 high angle reflections. The data collection and refinement parameters are presented in Table 6. The structure was solved by direct methods using SIR,[11] and refined by full-matrix least-squares methods using SHELXL.[12] All non-hydrogen atoms were refined anisotropically. Hydrogen atoms were placed in calculated positions. The largest unassigned peak in the final difference map was 0.51e/Å^3, located near the Ru ion. No absorption correction was applied. The structure was refined to a final *R* value of 7.52%. The refined cation is shown in Figure 2, and structural details are presented in Table 1.

X-ray Determination of [(bpy)$_2$Ru(2,2′-bipyridine-3,3′-19-crown-5)](PF$_6$)$_2$

A deep red, rectangular plate, approximately 0.25 × 0.25 × 0.12 mm, crystallized from an aqueous solution of the crown complex on standing. The crystal was chosen by size, habit, and polarized light microscopy. The complex also crystallized in the triclinic system in the space group $P\bar{1}$. The structure was solved by direct methods using SIR, and refined by full-matrix least-squares methods using SHELXL. All non-hydrogen atoms were refined anisotropically. Hydrogen atoms were placed in calculated positions. The largest unassigned peak in the final difference map was 0.8 e/Å^3, located near a PF$_6$ anion. No absorption correction was applied. Two waters of crystallization were observed. The structure was refined to a final *R* value of 7.41%. The refined cation is shown in Figure 2, and structural details are presented in Table 2.

In both complexes, the Ru−N bond lengths and angles are typical of a ruthenium diimine, spanning a range from 2.04 to 2.08Å. The two non-crown containing bipyridine rings in both complexes are flat to within 5°. However, the bipyridine containing the tethered crown ether was distorted by about 35° for the 4-oxygen crown, and by 24° for the 5-oxygen crown. As we expected, the presence of the crown ethers caused a geometric distortion at the ruthenium center. The magnitude of the distortion reflects the flexibility in the tethered crown ether. We were unable to obtain satisfactory crystals for the 6-oxygen crown complex.

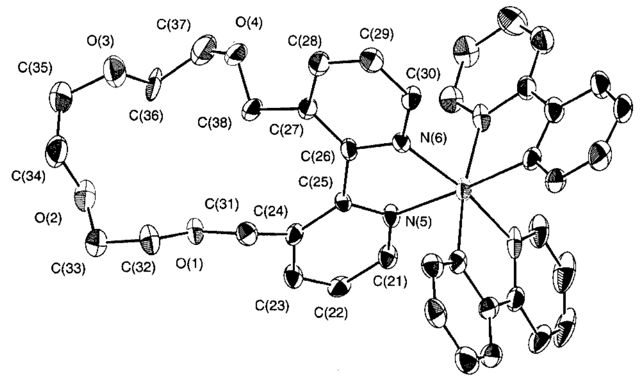

A. [(bpy)$_2$Ru(bpy-16-crown-4)]$^{2+}$

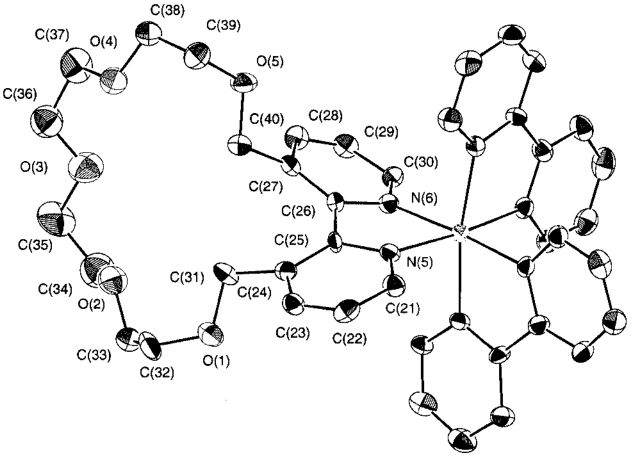

B. [(bpy)$_2$Ru(bpy-19-crown-5]$^{2+}$

Figure 2. ORTEP diagram of [(bpy)$_2$Ru(bpy-16-crown-4]$^{2+}$ (**A**) and [(bpy)$_2$Ru(bpy-19-crown-5]$^{2+}$ (**B**)

Electrochemistry

Half-wave potentials were determined by cyclic voltammetry (Figure 3) and are listed in Table 3. The cyclic voltammograms of each of the three [Ru(bpy)$_2$(crowns)]$^{2+}$ complex cations in CH$_3$CN exhibit one reversible Ru^{II}/Ru^{III} wave at a slightly lower potential than that observed for [Ru(bpy)$_3$]$^{2+}$. Three reversible reduction waves are also observed, with no significant shift in their positions relative to [Ru(bpy)$_3$]$^{3+}$. These data suggest that the slight twist of the inter-pyridine rings on the crown ligands does not alter the ground state electronics of the aromatic ring system, although the loss in angular overlap between the ligand and the ruthenium atom may slightly raise the energy of the ruthenium d-orbitals.

Emission Spectroscopy

The luminescence spectra for the three ruthenium crown complexes are also typical for ruthenium(II) *tris*-bipyridine analogs. At room temperature, the broad charge transfer spectra for the three complexes show little dependence on

Table 1. Selected bond lengths [Å] and angles [deg] for $[(bpy)_2Ru(bpy\text{-}16\text{-}crown\text{-}4)]^{2+}$

C(1)−C(12)	1.525(13)	C(1)−O(4)	1.381(12)
C(2)−C(3)	1.52(2)	C(2)−O(4)	1.419(14)
C(3)−O(3)	1.447(14)	C(4)−C(5)	1.44(2)
C(4)−O(3)	1.45(2)	C(5)−O(2)	1.445(15)
C(6)−C(7)	1.488(15)	C(6)−O(2)	1.421(14)
C(7)−O(1)	1.408(10)	C(8)−C(17)	1.507(12)
C(8)−O(1)	1.416(10)	C(11)−C(12)	1.404(11)
C(11)−C(16)	1.462(10)	C(11)−N(2)	1.384(9)
C(12)−C(13)	1.382(13)	C(13)−C(14)	1.402(14)
C(14)−C(15)	1.348(12)	C(15)−N(2)	1.329(11)
C(16)−C(17)	1.402(11)	C(16)−N(1)	1.368(9)
C(17)−C(18)	1.390(12)	C(18)−C(19)	1.356(12)
C(19)−C(20)	1.368(12)	C(20)−N(1)	1.327(10)
N(1)−Ru(1)	2.076(6)	N(2)−Ru(1)	2.079(6)
N(4)−Ru(1)	2.071(7)	N(3)−Ru(1)	2.038(7)
N(5)−Ru(1)	2.052(8)	N(6)−Ru(1)	2.039(7)
bond angles			
N(1)−Ru(1)−N(2)	79.1(2)	N(1)−Ru(1)−N(4)	176.0(2)
N(1)−Ru(1)−N(3)	100.6(3)	N(1)−Ru(1)−N(5)	93.1(3)
N(1)−Ru(1)−N(6)	87.0(3)	N(2)−Ru(1)−N(4)	96.9(3)
N(2)−Ru(1)−N(3)	86.8(3)	N(2)−Ru(1)−N(5)	172.1(3)
N(2)−Ru(1)−N(6)	98.5(3)	N(4)−Ru(1)−N(3)	78.5(3)
N(4)−Ru(1)−N(5)	90.9(3)	N(4)−Ru(1)−N(6)	94.2(3)
N(3)−Ru(1)−N(5)	96.2(3)	N(3)−Ru(1)−N(6)	171.5(3)
N(5)−Ru(1)−N(6)	79.5(3)		

Table 2. Selected bond lengths [Å] and angles [deg] for $[(bpy)_2Ru(bpy\text{-}19\text{-}crown\text{-}5)]^{2+}$

C(21)−C(22)	1.351(13)	C(21)−N(5)	1.321(11)
C(22)−C(23)	1.360(14)	C(23)−C(24)	1.399(14)
C(24)−C(25)	1.410(12)	C(24)−C(31)	1.517(14)
C(25)−C(26)	1.497(12)	C(25)−N(5)	1.367(10)
C(26)−C(27)	1.397(12)	C(26)−N(6)	1.366(11)
C(27)−C(28)	1.404(13)	C(27)−C(40)	1.514(12)
C(28)−C(29)	1.368(15)	C(29)−C(30)	1.369(13)
C(30)−N(6)	1.348(11)	C(31)−O(1)	1.410(12)
C(32)−C(33)	1.50(2)	C(32)−O(1)	1.393(14)
C(33)−O(2)	1.42(2)	C(34)−C(35)	1.47(3)
C(34)−O(2)	1.43(2)	C(35)−O(3)	1.40(2)
C(36)−C(37)	1.50(2)	C(36)−O(3)	1.41(2)
C(37)−O(4)	1.43(2)	C(38)−C(39)	1.50(2)
C(38)−O(4)	1.395(15)	C(39)−O(5)	1.422(13)
C(40)−O(5)	1.431(12)	N(1)−Ru(1)	2.073(6)
N(2)−Ru(1)	2.062(7)	N(3)−Ru(1)	2.072(7)
N(4)−Ru(1)	2.056(6)	N(5)−Ru(1)	2.062(7)
N(6)−Ru(1)	2.066(7)		
Bond angles			
N(1)−Ru(1)−N(3)	93.9(2)	N(1)−Ru(1)−N(2)	89.6(2)
N(1)−Ru(1)−N(5)	96.0(2)	N(1)−Ru(1)−N(4)	79.1(3)
N(2)−Ru(1)−N(3)	78.7(3)	N(1)−Ru(1)−N(6)	174.5(2)
N(2)−Ru(1)−N(5)	174.3(3)	N(2)−Ru(1)−N(4)	95.7(3)
N(3)−Ru(1)−N(4)	171.1(3)	N(2)−Ru(1)−N(6)	95.6(3)
N(3)−Ru(1)−N(6)	88.6(3)	N(3)−Ru(1)−N(5)	99.7(3)
N(4)−Ru(1)−N(6)	98.9(3)	N(4)−Ru(1)−N(5)	86.6(3)
N(5)−Ru(1)−N(6)	78.8(3)		

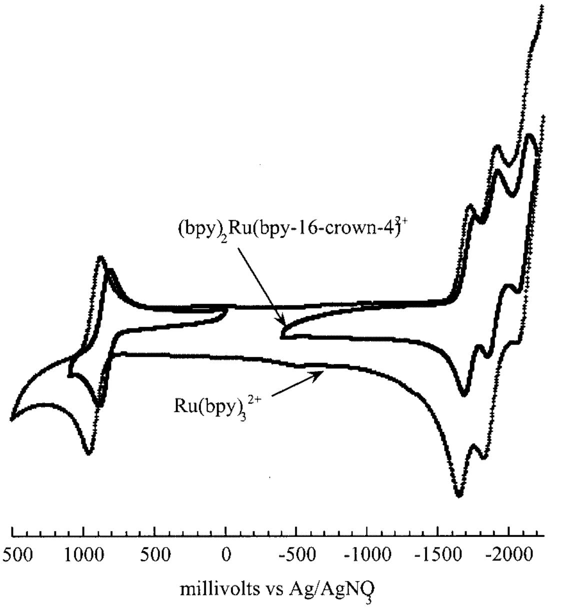

Figure 3. Cyclic voltammogram of the Ru complexes in acetonitrile

Table 3. Electrochemical data[a] for $Ru(bpy)_2(crown)^{2+}$ complexes

Ru(bpy)2(crown)	$Ru^{II/III}$ [mV]	bpy/bpy$^-$ [mV]		
2,2′-bipyridine-3,3′-16-crown-4	0.856	−1.71	−1.88	−2.09
2,2′-bipyridine-3,3′-19-crown-5	0.90	−1.75	−1.95	−2.15
2,2′-bipyridine-3,3′-21-crown-6	0.88	−1.70	−1.90	−2.12

the size of the tethered crown ether. At 77 K, only the 6-oxygen crown shows a small red shift in emission. The activation energies for the three complexes are within experimental error of each other (Table 4). The addition of Pb^{2+} ions to the complexes results in a small, but significant, increase in the emission intensity, but no significant change in the emission energy. The change in emission intensity for the three ligand complexes are similar and a typical response is shown in Figure 4. This result differs from that observed for $[(bpy)_2Ru(2,2'\text{-bipyridine-}3,3'\text{-}16\text{-crown-}4)]^{2+}$ in the presence of Group I metal ions.[13] However, it is not clear to what extent ion pairing impacts the observed emission behavior. We have observed that varying the concentration of the perchlorate ion causes shifts in the emission spectrum, similar to those previously reported.[14] For the results discussed here, the measurements were performed in DMSO/water solutions at constant ionic strength. Plotting the magnitude of the emission change over an extended range of Pb^{2+} concentrations yields a Ru−Pb complex stoichiometry of 1:1, with an equilibrium constant of $K \approx 0.4\ \text{M}^{-1}$.

NMR Spectroscopy

We examined the NMR spectra of the free ligands and the ruthenium complexes with and without additional metal ions such as Li^+, Na^+, K^+, Pb^{2+}, and Cs^+, in order to correlate the photophysical behavior of the ruthenium complexes with any geometric changes caused by the presence of the metal ions. Typically, a large excess of the allos-

Table 4. Photophysical data in DMSO/water

Complex[b]	λ_{max}, nm		Lifetime		E_a	Φ_{em}[a]	
	77 K	298 K	τ_{77}, μs	τ_{298}, ns	cm^{-1}	77 K	298 K
$(bpy)_2Ru(2,2'$-bipyridine-3,3'-16-crown-4$)^{2+}$	589	615	3.0	680	1950	0.0332	0.0138
$(bpy)_2Ru(2,2'$-bipyridine-3,3'-19-crown-5$)^{2+}$	588	617	3.3	700	2260	0.0321	0.0198
$(bpy)_2Ru(2,2'$-bipyridine-3,3'-21-crown-6$)^{2+}$	585	622	3.4	750	2520	0.0399	0.0174

[a] Quantum yields were determined by comparing the integrated intensity of the samples to that of an absorbance-matched standard, $[Ru(bpy)_3]^{2+}$ $\Phi = 0.062$. I. Dupry, T. J. Meyer, *Inorg. Chem.* **1996**, *35*, 6299. [b] DMSO/water used because of its low temperature glass properties. Results in CH_3CN are the same to within experimental error.

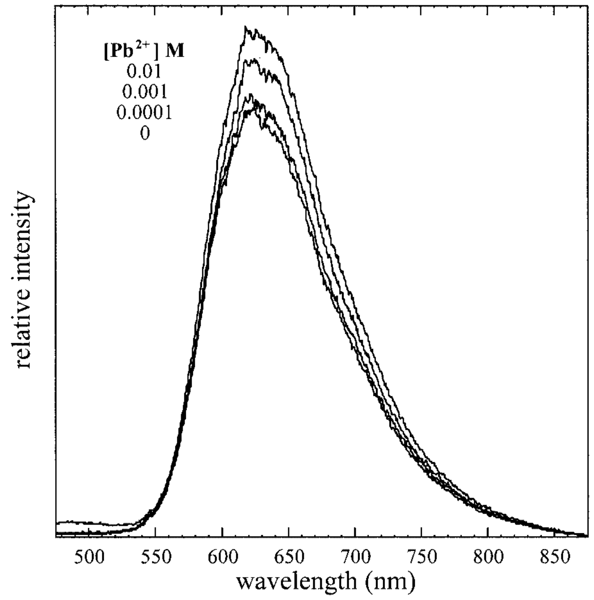

Figure 4. Emission spectrum of $(bpy)_2Ru(2,2'$-bipyridine-3,3'-16-crown-4$)^{2+}$ at room temperature with variable $[Pb^{2+}]$

teric ions, as their metal triflates, were added to the solution of $[Ru(bpy\text{-}crown)]^{2+}$ in $CDCl_3$ and/or [D$_6$]acetone so that any equilibria present would be shifted towards the products.

The NMR spectra of the crown ethers and their ruthenium complexes have two distinct spectral features that are well-separated: the aromatic region corresponding to the bipyridine moiety of the molecule (7−9 ppm), and the aliphatic (methylene) portion of the cyclic ethers (≈ 3−5.5 ppm). As an uncoordinated molecule, the bipyridine rings are twisted such that they are *anti* to each other with respect to the pyridine−pyridine bond. On coordination to the ruthenium atom via the pyridine nitrogen atoms, the benzylic protons are forced into close proximity. The resulting anisotropic field causes an AB splitting pattern in the benzylic resonances. As has been previously reported for the free ligands,[18] we observed that all regions of the ^{1}H spectrum undergo considerable changes on addition of Li^+, Na^+, K^+, Pb^{2+}, and Cs^+ ions. The most dramatic changes occur in the aromatic region, followed by a smaller change in the benzylic region, and finally a relatively small change in the region of the methylene groups. However, in the case of the ruthenium complexes, a different behavior is observed. For these complexes, essentially no change is seen in the aromatic region and very small changes in the methylene resonances. The largest change is observed for the resonances of the benzylic protons. For example, $[(bpy)_2Ru(2,2'$-bipyridine-3,3'-19-crown-5$)]^{2+}$ shows two doublets assigned to the benzylic protons 8a-H and 8b-H, at $\delta = 4.47$ and 4.73 ppm, respectively (Figure 5 and Table 5). In the presence of Pb^{2+} ions, these two resonances shift to $\delta = 4.63$ and 4.72 ppm, respectively. The coupling constant ($J_{8a\text{-}H-8b\text{-}H}$) decreases from 12.4 to 12.1 Hz. This indicates that the Pb^{2+} ion is interacting with the crown ether oxygen atoms, but that the interaction is not telegraphed to the bipyridine ring system. Similar results were observed for the 5-crown and 6-crown complexes in the

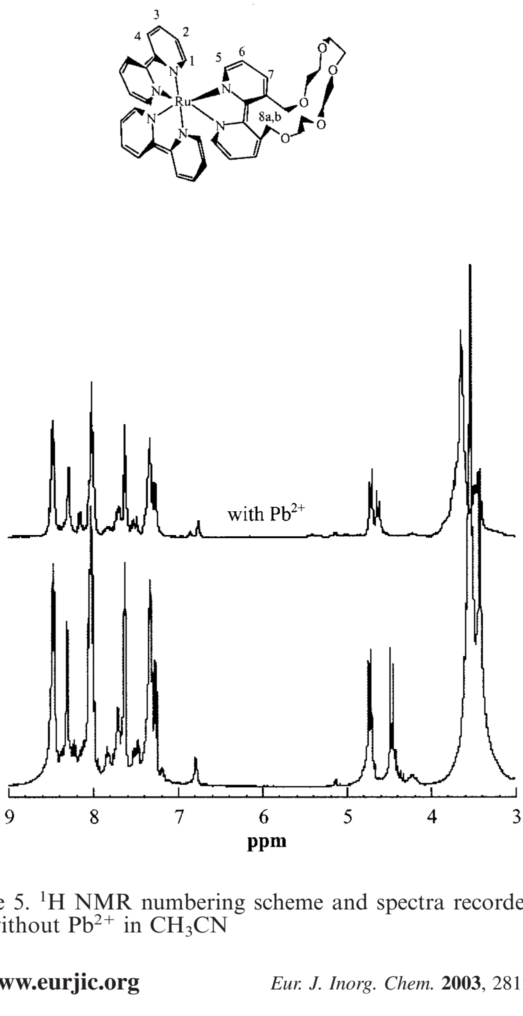

Figure 5. ^{1}H NMR numbering scheme and spectra recorded with and without Pb^{2+} in CH_3CN

Table 5. ^{1}H chemical shifts (ppm) of Ru Complexes in [D$_3$]acetonitrile with and without Pb^{2+}

Compound	Pb^{2+}	Chemical shift[a]										
		H1	H2	H3	H4	H5	H6	H7	H8a	H8b	Ether CH_2	
$(bpy)_2Ru(16\text{-crown-}4)^{2+}$		8.58 (d)	8.15 (m)	7.40	7.75	8.42 (d)	7.45	8.13 (m)	5.23 (d)	4.35 (d)	3.87 (b)	3.73 (b)
$(bpy)_2Ru(16\text{-crown-}4)^{2+}$	·	8.58 (d)	8.15 (m)	7.40	7.75	8.42 (d)	7.45	8.12 (m)	5.20 (d)	4.32 (d)	3.95 (b)	3.75 (b)
$(bpy)_2Ru(19\text{-crown-}5)^{2+}$		8.48 (d)	8.04 (m)	7.27	7.62	8.31 (d)	7.33	8.01	4.73 (d)	4.47 (d)	3.53 (b)	3.43 (b)
$(bpy)_2Ru(19\text{-crown-}5)^{2+}$	·	8.50 (d)	8.03 (m)	7.27	7.63	8.29 (d)	7.32	8.00 (m)	4.72 (d)	4.63 (d)	3.70 (b)	3.44 (b)
$(bpy)_2Ru(21\text{-crown-}6)^{2+}$		8.59 (m)	8.15 (m)	7.37	7.73	8.40 (m)	7.42	8.11 (m)	4.76 (m)	4.32 (b)	3.65 (b)	3.17 (b)
$(bpy)_2Ru(21\text{-crown-}6)^{2+}$	·	8.49 (m)	8.05 (m)	7.36	7.70	8.30 (m)	7.60	8.00 (m)	5.11 (m)	4.75 (m)	3.81 (b)	3.62 (b)

[a] Chemical shifts were assigned based on the ^{1}H-^{1}H COSY spectra.

presence of Pb^{2+} ions. The NMR shifts are substantially smaller for the other cations examined.

Conclusions

The smaller than expected, and previously observed,[9] photophysical response of the ruthenium crown complexes when exposed to Pb^{2+} ions is the result of stereochemical constraints exerted by the tethered crown ethers on their host bipyridine. Molecular modeling shows that in the ruthenium crown complexes, the protons on the benzylic carbon atoms (8a-,8b-H in Figure 5) are the major source of steric repulsion. These protons restrict the ability of the two pyridine rings from approaching co-planarity to less than about 15°. Regardless of the number of oxygen atoms in the ring, the oxygen atoms attached to the benzylic carbons are always positioned such that their lone pairs are no longer pointing inward towards the crown cavity.[14,15] In this way it is impossible for these two oxygen atoms to coordinate a guest ion. As the crown ring size increases, additional oxygen atoms are available to coordinate guest ions. However, these oxygen atoms are sufficiently removed from the bipyridine so as to offer little or no leverage for an allosteric perturbation of the ruthenium coordination sphere, since the flexibility of the crown framework is substantial. This, coupled with the proximity of the benzylic protons, prohibits any substantial change in the bipyridine ring geometry or motion. Without a substantial impact on the coordinated bipyridine, either in terms of geometry or electronics, no photophysical change is possible. We have prepared analogous crown complexes where the crowns are tethered directly to aromatic rings at the 3,3′ positions without a benzylic carbon and the problematic protons. The results of those studies will be reported elsewhere.

Experimental Section

Syntheses: All chemicals used were of reagent grade, or better, and used without further purification. The bipyridine crown-ether ligands 2,2′-bipyridine-3,3′-16-crown-4, 2,2′-bipyridine-3,3′-19-crown-5, 2,2′-bipyridine-3,3′-21-crown-6, and [*cis*-$(bpy)_2RuCl_2$]·$2H_2O$[16] were prepared by literature methods.[17] Metal triflates were prepared by treating the metal carbonates with neat CF_3SO_3H, (3M FC-43, technical grade), followed by recrystallization from dichloromethane.

Preparation of [$(bpy)_2Ru$(2,2′-bipyridine-3,3′-16-crown-4)]$(PF_6)_2$: [$Ru(bpy)_2Cl_2$]·$2H_2O$ (0.43 g) was added to an ethanolic solution of 2,2′-bipyridine-3,3′-16-crown-4 (0.27 g in 20 mL) in a 50-mL flask. The mixture was refluxed for 24 h, and was filtered when it was still hot. Ammonium hexafluorophosphate was added to the cooled filtrate, and the mixture was stored in a refrigerator overnight. The resulting orange−yellow precipitate was collected by filtration, washed with ether (30 mL), then dried under vacuum. The compound was purified by column chromatography (2 × 25 cm) on neutral alumina using an acetone/CH_2Cl_2 (4:7) mixture as the eluent. The first fraction was evaporated to near dryness and dissolved in a minimum volume of water. Addition of solid NH_4PF_6, followed by overnight refrigeration resulted in 500 mg of a crystalline product (86%yield). UV/Vis in (1:1) DMSO/0.1 M $NaCF_3SO_3$ [λ nm, ε (mol^{-1}cm^{-1})]: 227 (61620), 290 (69714), 450 (13950). ^{1}H NMR ([D$_6$]acetone): δ = 8.78 (d), 8.20 (m), 7.97 (m), 7.54 (m), 5.20, 4.50, 3.80, 3.70 ppm. ^{13}C NMR ([D$_6$]acetone): δ = 152.2 ppm, 138.0, 127.8, 72.0, 70.4, 70.1, 69.5. MS: *m*/*z* = 889, 372, corresponding to a monocation PF_6 salt and the parent dication, respectively.

Preparation of [$(bpy)_2Ru$(2,2′-bipyridine-3,3′-19-crown-5)]$(PF_6)_2$: This compound was synthesized and purified following the same procedure as that described for the 2,2′-bipyridine-3,3′-16-crown-4 complex. Reacting 0.25 g of the crown ligand resulted in 512 mg of the ruthenium complex. (91.9% yield). UV/Vis in (1:1) DMSO/0.1 M $NaCF_3SO_3$ [λ nm, ε (mol^{-1}cm^{-1})]: 236 (78126), 290 (40660), 450 (6460). ^{1}H NMR ([D$_6$]acetone): δ = 8.8 (d), 8.2 (m), 8.00 (m), 7.55 (m), 4.92, 4.70, 3.65, 3.00 ppm. ^{13}C NMR ([D$_6$]acetone): δ = 157.5 ppm, 152.2, 137.8, 127.6, 126.8, 71.0−69.0(5 peaks). MS: *m*/*z* = 395.

Preparation of [$(bpy)_2Ru$(2,2′-bipyridine-3,3′-21-crown-6)]$(PF_6)_2$: This compound was synthesized and purified following the same procedure as that described for the 2,2′-bipyridine-3,3′-16-crown-4 complex, without significant modification, except that acetone was used as the eluent. Reacting 0.31 g of the crown ligand resulted in 496 mg of the ruthenium complex. (76.2% yield). UV/Vis in (1:1) DMSO/0.1 M $NaCF_3SO_3$ [λ nm, ε (mol^{-1}cm^{-1})]: 236 (30878), 290 (69714), 450 (13950). ^{1}H NMR ([D$_6$]acetone): δ = 8.8 (d), 8.20 (m), 8.00 (m), 7.50 (m), 5.00, 3.65, 3.55 ppm. ^{13}C NMR ([D$_6$]acetone): δ = 152.3 ppm, 138.5, 127.8, 124.8, 68.1−70.0. MS: *m*/*z* = 416.

Physical Measurements

Spectroscopic Measurements: IR spectra were recorded using KBr pellets on a Perkin−Elmer 1710 FTIR or a Bruker Equinox 55 FTIR. UV/Vis spectra were recorded on a Beckman 7400 diode array spectrometer. NMR spectra were recorded on a JEOL Eclipse+ 400 multinuclear NMR (400 MHz ^{1}H) equipped with a *z*-axis gradient probe. Luminescence spectra were recorded on a

Table 6. Data collection and refinement parameters for $[(bpy)_2Ru(bpy\text{-}16\text{-}crown\text{-}4](PF_6)_2$ and $[(bpy)_2Ru(bpy\text{-}19\text{-}crown\text{-}5](PF_6)_2$

	$[(bpy)_2Ru(bpy\text{-}16\text{-}crown\text{-}4)](PF_6)_2$	$[(bpy)_2Ru(bpy\text{-}19\text{-}crown\text{-}5)](PF_6)_2$
Space group	$P\bar{1}$	$P\bar{1}$
Cell constants	a = 12.5404(0.0025) Å	a = 12.7320(0.0039) Å
	b = 12.6871(0.0047) Å	b = 13.0510(0.0043) Å
	c = 14.4495(0.0059) Å	c = 14.0350(0.0054) Å
	α = 101.2932(0.0330)°	α = 86.186(0.0288)°
	β = 102.6826(0.0161)°	β = 77.326(0.0282)°
	γ = 93.0886(0.0230)°	γ = 86.99(0.0255)°
Reflections collected	$0 < h > 12$	$0 < h > 15$
	$-13 < k > 13$	$-15 < k > 15$
	$-17 > l > 16$	$-16 > l > 16$
No. of reflections (total/unique/I_0>4$\Sigma(I_0)$]	7560/7359/4579	7737/7687/4626
Scan method	$\omega/2\theta$	$\omega/2\theta$
Empirical formula	$C_{38}H_{38}F_{12}N_6O_4P_2Ru$	$C_{40}H_{46}F_{12}N_6O_8P_2Ru$
Formula mass	1033.74 amu	1166.24 amu
Formula units per cell	$Z = 2$	Z = 2
Density	$d_{calcd.} = 1.594$ g/cm^{-3}	$d_{calcd.} = 1.631$ g/cm^{-3}
Absorption coeff.	$\mu = 0.54$ mm^{-1}	$\mu = 0.52$ mm^{-1}
Temperature	$T = 295$ K	$T = 295$ K
Radiation (Mo-K_{α})	$\lambda = 0.7107$ Å	$\lambda = 0.7107$ Å
F_{000}	1044 e	1116 e
Structural parameters	571	607
R_1	0.0752	0.0865
wR_2	0.2075[a]	0.2373[a]

[a] Weight = $([\Sigma^2(F_o^2) + (0.1183\cdot P)^2 + 7.99\cdot P])^{-1}$ where $P = [\max(F_o^2,0) + 2F_c^2]/3$. [a] Weight = $([\Sigma^2(F_o^2) + (0.1081\cdot P)^2 + 7.99\cdot P])^{-1}$ where $P = [\max(F_o^2,0) + 2F_c^2]/3$.

PTI Quanta Master spectrometer. Spectra were corrected for wavelength response and lamp intensity fluctuations. Mass spectra were obtained from a Micromass QUATTRO II mass spectrometer by direct insertion.

Photophysical Measurements: Quantum yield determinations were performed using nitrogen purged, absorbance matched (0.1 A @450 nm) samples in DMSO/water (1:1 v/v) solutions. $[Ru(bpy)_3]^{2+}$ was used as the standard. Luminescent lifetimes were determined by exciting the samples with the third harmonic from a Continuum Surelite-I Nd:YAG laser. The laser was run at minimum flash lamp power and the beam was attenuated so that sample irradiation occurred with a less than 100 μJ/10 ns pulse @355 nm. The emitted light was filtered with a 450 nm cut-off filter to eliminate laser scatter, and collected by a fiber optic interfaced to an Acton SP300i monochromator/Hamamatsu R928 PMT. The photomultiplier was run at a constant −1000 V, and the light level was adjusted using the monochromator slits in order to provide a signal no larger than 100 mV across 50 W. Typically 16 transients were recorded on a LeCroy LT342 DSO, and the data fit by non-linear least-squares methods. Sample temperatures were maintained to ±0.5 K with an Oxford Optistat liquid-nitrogen cryostat. All device control and data manipulations were performed with a computer program developed in-house. Variable temperature lifetime data were fit to an Arrhenius function for the determination of activation energies.

Electrochemical Data: Cyclic voltammograms were recorded in nitrogen purged CH_3CN at room temperature, using a BAS 50 W potentiostat equipped with a Pt working and auxiliary electrodes and an $Ag/AgNO_3$ reference electrode. Tetrabutylammonium perchlorate was used as the supporting electrolyte.

X-ray Structure Data: Single crystal data (Table 6) were recorded on a Nonius CAD4 diffractometer at −100 °C by using graphite-monochromated Mo-$K\alpha$ radiation. The crystal was mounted on a glass fiber with epoxy and placed with a random orientation on the diffractometer. The unit cell and data collection parameters were determined from 25 high angle reflections. The space group and structural parameters were determined using the maXus suite of programs. Intensity standards were recorded after each 100 minutes of exposure.

CCDC-198711 for $[(bpy)_2Ru(bpy\text{-}16\text{-}crown\text{-}4)](PF_6)_2$ and CCDC-198712 for $[(bpy)_2Ru(bpy\text{-}19\text{-}crown\text{-}5)](PF_6)_2$ contain the supplementary crystallographic data for this paper. These data can be obtained free of charge at www.ccdc.cam.ac.uk/conts/retrieving.html [or from the Cambridge Crystallographic Data Centre, 12, Union Road, Cambridge CB2 1EZ, UK; Fax: (internat.) +44-1223/336-033; E-mail: deposit@ccdc.cam.ac.uk].

Acknowledgments

Support for this research was generously provided by the National Science Foundation (CHE-9876142), the Kalamazoo Foundation and Western Michigan University.

---

[1] Portions of this manuscript were submitted in partial fulfillment for the degree of Master of Arts, Western Michigan University, **1999**.

[2] See the excellent series of reviews in: L. Fabbrizzi (Ed.), *Coord. Chem. Rev.* **2000**, vol. *205*, pp. 3−228.

[3] A. W. Czarnick (Ed.), *Fluorescent Chemosensors for Ion and Molecule Recognition*; American Chemical Society: Washington DC, ACS Symposium Series 538, **1992**.

[4] A. P. de Silva, H. Q. Gunaratne, T. Gunnlaugsson, A. J. Huxley, C. P. McCoy, J. T. Rademacher, T. E. Rice, *Chem. Rev.* **1997**, *97*, 1515.

[5] [5a] O. S. Wolfbeis (Ed.), *Fiber Optic Chemical Sensors and Biosensors*; CRC Press: Boca Raton, Florida, **1991**, vol. I & II. [5b] R. A. Bissell, A. P. de Silva, H. Q. N. Gunaratne, P. L.

Lynch, G. E. M Maguire, C. P. McCoy, K. R. A. S. Sandanayake, *Chem. Soc. Rev.* **1992**, *21*, 187. [5c] R. A. Bissell, A. P. de Silva, H. Q. N. Gunaratne, P. L. Lynch, G. E. M. Maguire, K. R. A. S. Sandanayake, *Top. Curr. Chem.* **1993**, *168*, 223. [5d] A. P. de Silva, H. Q. Gunaratne, T. Gunnlaugsson, A. J. M. Huxley, C. P. McCoy, J. T. Rademacher, T. E. Rice, *Adv. Supramol. Chem.* **1997**, *4*, 127.

[6] [6a] V. Balzani, F. Scandola, *Supramolecular Photochemistry*; Ellis−Horwood: Chichester, **1991**. [6b] V. Balzani, A. Credi, F. Scandola, "Supramolecular Photochemistry and Photophysics. Energy-Conversion and Information-Processing Devices Based on Transition Metal Complexes" in: *Transition Metals in Supramolecular Chemistry* (Eds.: L. Fabbrizzi, A. Poggi), Kluwer: Dorecht, **1994**. [6c] “Perspectives in Supramolecular Chemistry-from Molecular Recognition towards Molecular Information Processing and Self-Organization”: J. M. Lehn, *Angew. Chem. Int. Ed. Eng.* **1990**, *29*, 1304. [6d] L. Fabbrizzi, A. Poggi (Eds.), *Transition metals in Supramolecular Chemistry*; Kluwer: Dorecht, **1994**.

[7] M. H. Keefe, K. D. Benkenstein, J. T. Hupp, *Coord. Chem. Rev.* **2000**, *205*, 201.

[8] [8a] W. Szulbinski, J. Kincaid, *Inorg. Chem.* **1998**, *37*, 859. [8b] M. Sykora, J. Kincaid, *Inorg. Chem.* **1995**, *34*, 5852. [8c] S. Bélanger, M. Gilbeertson, D. Yoon, C. Stern, X. Dang, J. Hupp, *J. Chem. Soc., Dalton* **1999**, *19*, 3407. [8d] L. Fabrizzi, A. Poggi, *Chem. Soc., Rev.* **1995**, *24*, 197. [8e] L. Fabrizzi, M. Licchelli, P. Pallavicini, D. Sacchi, A. Taglietti, *Analyst* **1996**, *121*, 1763.

[9] M. W. Perkovic, *Inorg. Chem.* **2000**, *39*, 4962.

[10] We have determined the X-ray structure of the four oxygen crown and calculated the geometry of the four, five and six oxygen crowns. In the solid state the four oxygen crown has an inter-pyridine angle of 87°. These results will be pubished elsewhere.

[11] *International Tables for X-ray Crystallography*; Kynoch: Birmingham, **1965**.

[12] *SIR92:* A. Altomore, G. Casscarano, C. Giacovazzo, A. Guggliandi, M. C. Burla, G. Polidori, G. M. Camalli, *J. Appl. Cryst.* **1994**, *27*, 435.

[13] G. Sheldrick, *SHELXL-97* crystal structure refinement package, Unix release 97-2.

[14] M. Chiba, K. Ogawa, K. Tsuge, M. Abe, H.-B. Kim, Y. Sasaki, N. Kitamura, *Chem. Lett.* **2001**, *7*, 692.

[15] J. Rebek, T. Costello, L. Marshall, R. Watley, R. C. Gadwood, K. Onan, *J. Am. Chem. Soc.* **1985**, *107*, 7481.

[16] S. V. Luis, J. C. Frías, M. I. Burguete, M. Bolte, *Acta Crystallogr., Sect. C* **1998**, *54*, 1093.

[17] B. P. Sullivan, D. J. Salmon, T. J. Meyer, *Inorg. Chem.* **1978**, *17*, 3334.

[18] J. Rebek Jr., J. E. Trend, R. V. Watley, A. Chakravorti, *J. Am. Chem. Soc.* **1979**, *101*, 4333.

Received November 27, 2002